EXPLORATION OF THIOPHENE-BASED DONOR-DONOR AND DONOR-ACCEPTOR CONJUGATED OLIGOMERS

by

Steven G. Owens

B.S. Chemistry, The Pennsylvania State University, 2009

Submitted to the Graduate Faculty of

the Kenneth P. Dietrich School of Arts and Sciences in partial fulfillment

of the requirements for the degree of

Master of Science

University of Pittsburgh

2013

UNIVERSITY OF PITTSBURGH

KENNETH P. DIETRICH SCHOOL OF ARTS AND SCIENCES

This thesis was presented

by

Steven G. Owens

It was defended on

August 12th 2013

and approved by

Geoffrey R. Hutchison, Assistant Professor, Department of Chemistry

Tara Y. Meyer, Associate Professor, Department of Chemistry

Jill Millstone, Assistant Professor, Department of Chemistry

Thesis Advisor: Geoffrey R. Hutchison, Assistant Professor, Department of Chemistry

EXPLORATION OF THIOPHENE-BASED DONOR-DONOR AND DONOR-ACCEPTOR CONJUGATED OLIGOMERS

Steven G. Owens, M.S.

University of Pittsburgh, 2013

Conjugated polymers are one of the leading technologies in electronic materials research. In this work we investigate thiophene-based donor-donor (D-D) and donor-acceptor (D-A) conjugated oligomers for future application towards polymer solar cells (PSCs).

Beginning from computational studies, our group targets specific monomers that show promise in both bandgap and solar cell efficiency. For this research, we have found a novel alkyl-nitrothiophene (2-bromo-5-cyano-3-hexyl-4-nitrothiophene, NT) monomer as well as a unique D-D combination of propylenedioxythiophene (ProDOT) and isothianapthene (ITN). In both of these cases, we found that we can tune the tetramer bandgap (in both D-D and D-A systems) simply by changing the order of monomers (rather than changing the identity of the monomers). Horner-Wadsworth-Emmons (HWE) was chosen to provide the ability to individually couple monomers, allowing us to synthesize sequenced oligomers.

The synthesis of the novel alkyl-NT monomer was successful and progress towards additional monomers necessary for HWE coupling was made. A test Stille coupling towards the synthesis of the ProDOT-ITN oligomer was also attempted.

TABLE OF CONTENTS

LIST OF FIGURES

LIST OF SCHEMES

1.0 INTRODUCTION

With global industrialization and population increases, the projected global energy demand in 2050 is twice what it is today.[1] With this increase in energy consumption comes the recognition that traditional fossil fuel based energy sources have a negative impact on our planet. Solar energy shows tremendous promise for meeting energy needs from renewable and clean sources. In 2011, 12.8% of annual energy generation in the U.S. came from renewable sources, with 1% of this being solar. Along with wind, solar photovoltaics (PVs) are the fastest growing. Solar generation grew by a factor of nine between 2000 and 2011, and in 2011 alone, PV capacity in the U.S. increased by more than 86%. Still, solar electricity only comprises 0.2% of overall U.S. energy generation.[2] In 2010, the total annual electricity sales in the U.S. totaled about 3,754 TWh. According to a Geographic Information Systems (GIS)-based analysis performed by the National Renewable Energy Laboratory (NREL) in 2012, U.S. urban PVs could generate 2,200 TWh and rural PVs 280,060 TWh.[3] By utilizing just 1-2% of the available rural space for PVs, the country's demand for energy could be satisfied. By increasing efficiency and reducing the cost of PVs by developing new technologies such as organic photovoltaics (OPVs), we can further decrease the land mass needed.

1.1 OPV HISTORY

The first OPV was reported in 1986 by Tang as a two-layer, small molecule cell.[4] Since that discovery, the field has advanced towards supplementing current inorganic silicon-based PVs with polymer solar cells (PSCs). PSCs provide many improvements over their inorganic counterparts including lower cost, ease of manufacturing (roll-to-roll and inkjet printing),

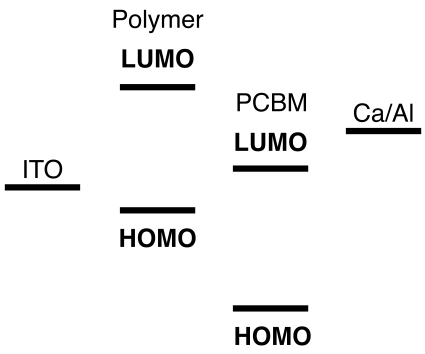

Figure 1.1: A energy level diagram showing the relative energies of the p-type polymer, n-type fullerene, and electrodes in a PSC.

high synthetic tailorability, and the ability to make large area, flexible, and transparent cells.[1,5–9] PSCs consist of a p-type conjugated polymer and an n-type fullerene. The conjugated polymer is typically composed of donor (easily oxidized) and acceptor (easily reduced) monomers, providing a narrow band gap and a good energy level match with the n-type fullerene (Figure 1.1).

Before the development of the two-layer (planar heterojunction) OPV in 1986, the standard was a single layer of an organic compound between two different electrodes. Tang's two-layer OPV consisted of copper phthalocyanine and a perylene tetracarboxylic derivative sandwiched between two electrodes (Figure 1.2a), where the interface was responsible for the majority of charge separation. While showing great improvement over the previous generation of OPVs, the thickness of the layers (and therefore number of photons absorbed) in the planar heterojunction cell are limited by the exciton diffusion length (10 nm).[10,11] When light is absorbed by either layer, excitons are generated which must then migrate to the interface between the layers before they can separate. With films thicker than the exciton diffusion length, recombination dominates because most of the generated excitons do not reach the interface. This problem was solved with the development of the bulk heterojunction (BHJ) architecture (Figure 1.2b) in 1992 by Sariciftci (poly[2-methoxy,5-(2'-ethyl-hexyloxy)-p-phenyl-ene vinylene (MEH-PPV) and C_{60})[12] and Morita (poly(3-alkylthiophene) (PAT)

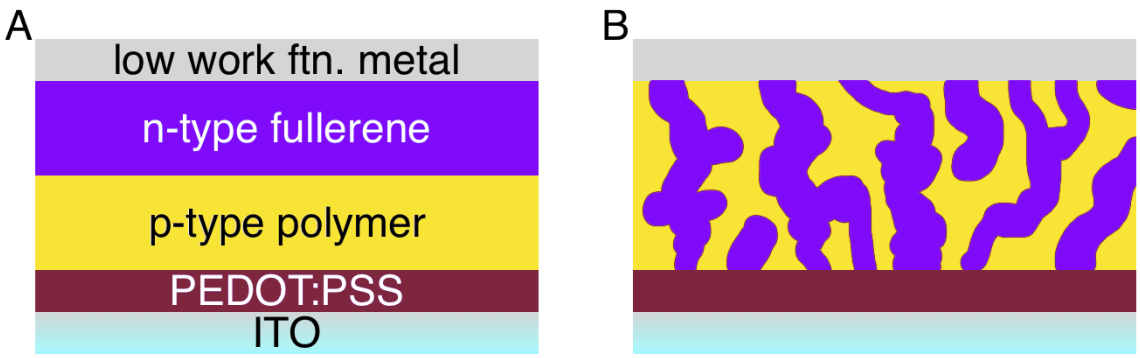

Figure 1.2: Typical device architecture for (a) planar heterojunction PSCs and (b) bulk heterojunction PSCs.

and C_{60}).[13] When BHJ active layer domains are kept within the exciton diffusion length, an efficient pathway for charge transport and collection is formed allowing for increased film thickness, thus overcoming the problems with the planar heterojunction architecture.[7,14] This also lead to the discovery of charge transfer from conjugated polymers to fullerenes on a picosecond time scale.[12,13] With the development of regeoregular poly(3-hexylhiophene) (RR-P3HT) in 1993 by by Rieke, et al. and McCullough, et al.,[15–17] P3HT became the most common p-type polymer used in PSCs. Since the mid 1990s, the PSC field has been an area of great interest and efficiency has increased from about 2% to 4-5% with P3HT a few years ago and is now pushing 11%, through the development of new low band gap polymers, tandem solar cells (multiple active layers), and small molecule absorbers.[1,18]

1.2 PSC DETAILS AND EFFICIENCY

PSCs generate current when light shines through the ITO cathode and the polymer absorbs photons (with energies corresponding to its bandgap), this generates bound electron-hole pairs (excitons). The fullerene can also absorb photons and generate excitons. The excitons diffuse towards the p-n junction where they separate into free charge carriers. Electrons are

transferred from the LUMO of the polymer to the LUMO of the fullerene and holes from the HOMO of the fullerene to the HOMO of the polymer.[19]

The n-type fullerene is well entrenched in the field with most devices using phenyl-C_{61}-butyric acid methyl ester ($PC_{61}BM$) or phenyl-C_{71}-butyric acid methyl ester ($PC_{71}BM$), with $PC_{71}BM$ having better visible light absorption.[11] This work is focused on optimizing the p-type conjugated polymer to increase the efficiency of PSCs. Some of the early and widely used p-type polymers include poly(*p*-phenylene vinylene) (PPV) derivatives such as MEH-PPV and MDMO-PPV and thophene derivatives such as P3HT.[6,7,9,19]

Solar cell efficiency is calculated by Equation 1.1 with P_{IN} being the input factor (or the incident light) and fill factor (FF) being determined by Equation 1.2.[6,8]

$$PCE = V_{OC} \times J_{SC} \times \frac{FF}{P_{IN}} \tag{1.1}$$

$$FF = \frac{|J_{max}|\, V_{max}}{|J_{SC}|\, V_{OC}} \tag{1.2}$$

J_{max} and V_{max} are obtained from the J-V curve of the PSC (Figure 1.3).

The open-circuit voltage (V_{OC}) is the energy difference between the HOMO of the polymer and the LUMO of the fullerene and can be calculated by Equation 1.3, where e is elementary charge and 0.3 eV represents the energy required to separate the electron and hole 1.0 nm in a given dielectric constant.[6]

$$V_{OC} = e^{-1} \times \left(\left| E_{HOMO}^{polymer} \right| - \left| E_{LUMO}^{fullerene} \right| - 0.3eV \right) \tag{1.3}$$

The V_{OC} drives the separation of the excitons and is the measured voltage when the current density is zero.[20] Short-circuit current density (J_{SC}) can be calculated by multiplying the external quantum efficiency (EQE, the percentage of incident photons converted to excitons) with the incident spectrum (the typical solar radiation on earth's surface is represented by the AM 1.5 model) and integrating and is the current density when the voltage across the device is zero.[20] From Equation 1.1, it can be seen that both V_{OC} and J_{SC} are proportional to the efficiency. We can also rationalize that a lower HOMO level in the polymer would increase V_{OC}, however, this would also increase the band gap, reducing the ability of the

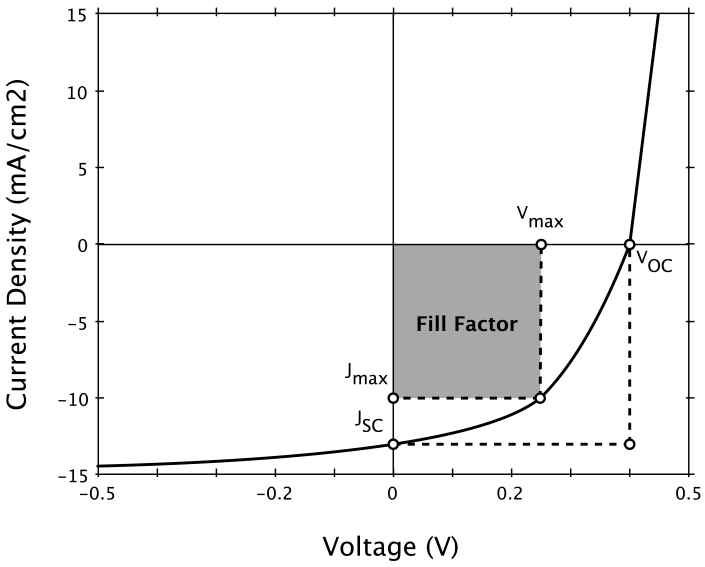

Figure 1.3: A sample J-V curve of a device in the dark (dashed line) and light (solid line) showing the experimental origins of V_{max}, J_{max}, V_{OC}, and J_{SC}.

polymer to absorb light, lowering J_{SC}.[8] In general, decreasing the band gap of the polymer increases J_{SC} and decreases V_{OC}, making it necessary to carefully select a polymer band gap to get optimal efficiency.[20]

There are many other issues to consider when choosing an appropriate polymer for a PSC. The optimal band gap for the p-type polymer is 1.4-1.6 eV.[21] This band gap gives the best balance between V_{OC} and J_{SC} and alignment with the solar spectrum for maximum photon absorption. Morphology, solubilizing side chains, size of solubilizing side chains, molecular weight, charge mobility, interchain distance, solubility with fullerene also all affect the properties of the polymer and efficiency of the PSC.[7,8,19,22,23]

Typically, the band gap of conjugated polymers is tuned by modifying monomers to change their donating and accepting abilities.[7,8,19,22,23] Polymers are typically in alternating, random, or block patterns, which do not necessarily provide the best optoelectronic properties. Previous work by this group has shown that is is possible to push the 10% efficiency barrier by targeting monomer sequence.[24] We call this the "sequence effect" and seek to

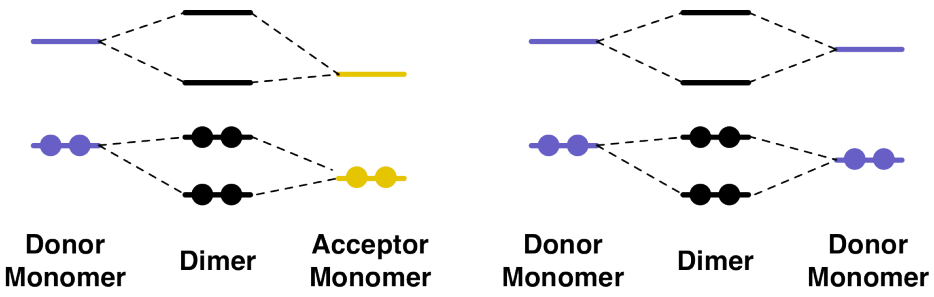

Figure 1.4: Energy level diagrams for D-A and D-D dimers.

modify polymer band gaps simply by changing monomer order in an oligomer or polymer.[25] This work focuses on the synthesis of new monomers for D-A conjugated polymers as well as investigating the properties of donor-donor (D-D) conjugated polymers. D-A and D-D polymers differ in how their electronic properties are derived from the individual monomers (Figure 1.4). While all energy levels are influenced by the energy levels of both monomers, in the D-A system, the HOMO energy of the dimer is most closely related to that of the donor monomer and the LUMO energy of the acceptor. In the case of the D-D system, the HOMO energy remains most closely related to that of the higher energy donor monomer while the LUMO energy is significantly lower than that of either donor monomer. This results in a lower band gap due to the higher delocalization of electrons. This high degree of delocalization may improve performance by increasing charge mobility and separation. We therefore believe that the D-D motif may be a promising new strategy for new p-type materials.

The goal of this work is to synthesize novel monomers (alkyl-nitrothiophene (NT)), investigate the D-D approach through synthesis (ProDOT-ITN), and use the results to elucidate the sequence effect. By comparing experimentally determined properties with those found *in silico*, we can find trends to predict good monomer candidates empirically.

2.0 INITIAL COMPUTATIONAL STUDIES

2.1 INTRODUCTION

Computational studies of molecules can help direct synthetic efforts to lessen the amount of time and resources wasted on compounds without the desired properties. In our group's computational work, we seek to study conjugated polymer monomers and oligomers to predict their energy levels and solar cell efficiency.[24,25] This chapter discusses an effort to computationally study how band gaps can be modified by simply changing the sequence of monomers in a tetramer.

2.2 D-A SEQUENCE EFFECT

The HOMO-LUMO gaps for a sequenced set of oligomers of phenylene vinylene-nitrothiophene vinylene (PV-NTV) were calculated and compared to the groups results for phenylene vinylene-phenylene vinylene (PV-PV) and phenylene vinylene-benzathiadiazole (PV-BDTV) (Figure 2.1). The NT monomer came from the groups previous computational screening.[24] Both the PV-BDTV (Figure 2.1b) and the PV-NTV (Figure 2.1c) oligomers span the full visible range, allowing the selection of a desired bandgap by simply changing the sequence.

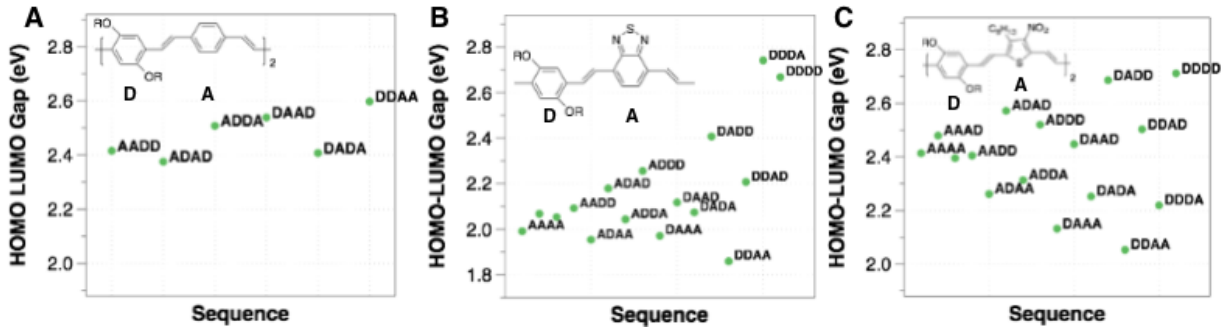

Figure 2.1: Comparison of DFT computed HOMO-LUMO gaps across a range of sequences for (a) PV-PV oligomers, (b) PV-BDTV oligomers, and (c) PV-NTV oligomers.

2.3 D-D SEQUENCE EFFECT

The D-D strategy for making novel oligomers and polymers for OPVs also emerged from the groups screening study.[24] Of the top (highest predicted solar efficiency) 25 oligomers in the study, almost all monomers were electron-donating. Many of the top oligomers were also not of the frequently used alternating $(ABAB)_n$ sequence.[24] I targeted two interesting D-D systems, propylenedioxythiophene-isothianapthene (ProDOT-ITN) (Figure 2.2a) and 3,4-ethylenedioxythiophene-isothianapthene (EDOT-ITN) (Figure 2.2b), investigating both computationally. Both sets of oligomers again show a 1 eV range in their HOMO-LUMO gaps, slightly redshifted in the visible spectrum compared to the D-A pairs. From these results, it became clear that it is possible to span the visible spectrum by varying the sequence of an oligomer chain, rather than modifying the monomers.

2.4 COMPUTATIONAL METHODS

All monomers were coded as SMILES, and a Python script utilizing Open Babel[26] (accessed through Pybel) was used to generate all possible tetramer combinations. Initial 3D structures of the tetramers were generated using Open Babel (through Pybel). The MMFF94[27–29]

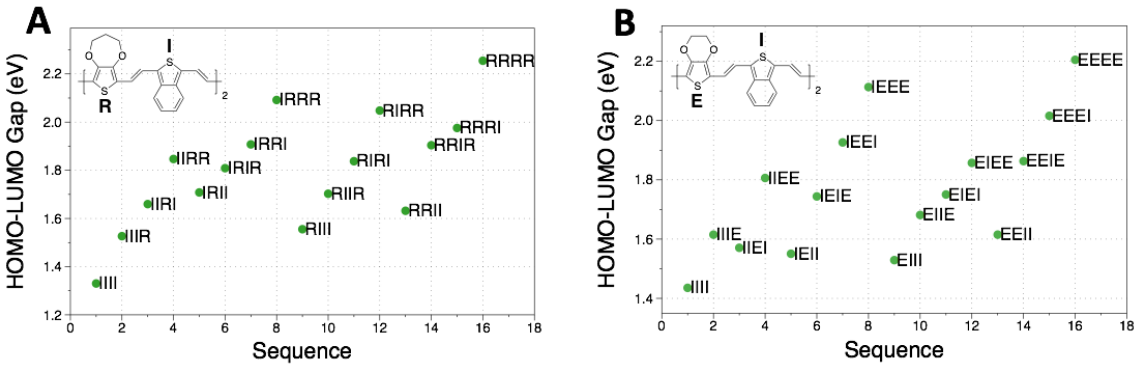

Figure 2.2: Comparison of DFT computed HOMO-LUMO gaps across a range of sequences for (a) ProDOT-ITN and (b) EDOT-ITN oligomers.

force field was used to perform a molecular mechanics minimization folowed by a stochastic Monte Carlo conformer search. This finds the lowest energy (most stable) conformer. Final geometry optimization was carried out using Gaussian 09[30] with density functional theory (DFT) and the B3LYP/6-31G(d) functional. While the HOMO and LUMO eigenvalues from DFT cannot be taken as the ionization potential or electron affinity, it has been demonstrated that they are linerally related to experimental electrochemical data.[31]

3.0 THIOPHENE MONOMERS AND THE NOVEL NITROTHOPHENE ACCEPTOR

3.1 INTRODUCTION

This chapter discusses the synthesis of the novel alkyl-nitrothiophene (NT) (**1**) monomer along with progress towards the other monomers necessary to test the PV-NTV motif from Chapter 2 experimentally. The PV-NTV oligomer takes advantage of the Horner-Wadsworth-Emmons (HWE) reaction. HWE chemistry allows for the formation of olefins from a reaction between a phosphonate and an aldehyde or ketone.[32] Utilizing the HWE reaction, sequence-directed oligomers can be built in a stepwise fashion, and has been developed by the Meyer group for coupling phenylene vinylenes (a sample coupling is shown in Figure 3.1).[33]

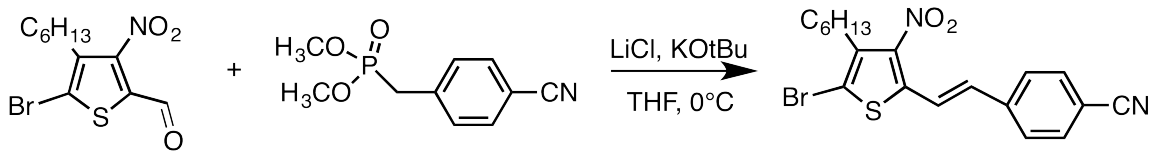

Figure 3.1: An example HWE coupling between NT and a vinylene monomer to form a PV-NTV motif.

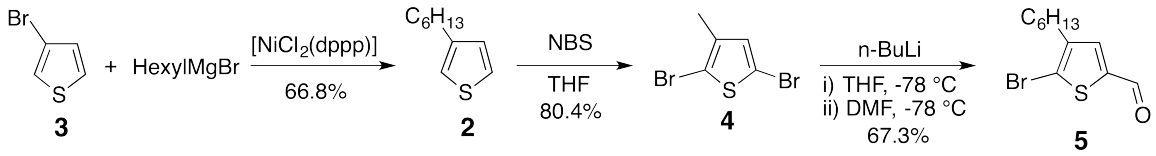

Scheme 3.1: Synthesis of 2-bromo-5-formyl-3-hexylthiophene.

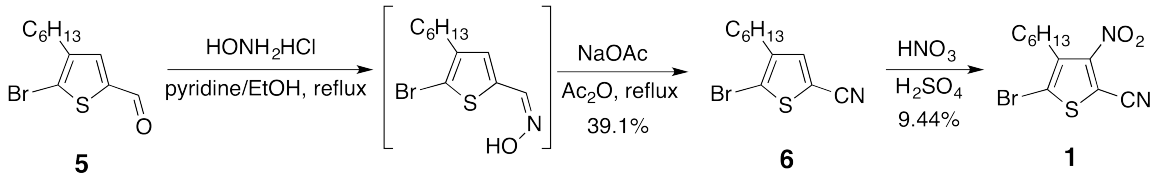

Scheme 3.2: Synthesis of 2-bromo-5-cyano-3-hexyl-4-nitrothiophene.

3.2 RESULTS AND DISCUSSION

The synthesis of 2-bromo-5-cyano-3-hexyl-4-nitrothiophene (**1**) was carried out mainly by literature procedures. 3-hexylthiophene (**2**) was synthesized from 3-bromothiophene (**3**) using a Stille coupling method from Loewe. Bromination of **2** to form 2,5-dibromo-3-hexylthiophene (**4**) was carried out with NBS, again using a method from Loewe.[34] The bromine at the 5-position of **4** was selectivly converted to an aldehyde using a method from Hayashi to form 2-bromo-5-formyl-3-hexylthiophene (**5**) (Scheme 3.1). Using a two step method (without isolation of the intermediate) from Hayashi, **5** is converted to 2-bromo-5-cyano-3-hexylthiophene (**6**).[35] The nitration of **6** to form **1** is carried out based on work by Mozingo, with significant modifications (Scheme 3.2).[36]

The main challenge in the preparation of **1** was in the nitration step (**6** to **1**). While many examples of nitrated-thiophenes are seen in the literature, many are not as highly substituted as NT. The electron-withdrawing cyano moiety reduces the activity of the unsubstituted 4-position on the thiophene ring. While the reduced activity poses a challenge, the extremely strong conditions provided by the mixture of con. H_2SO_4, fuming H_2SO_4, and fuming HNO_3

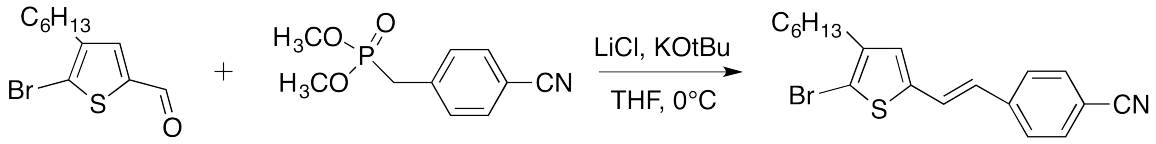

Scheme 3.3: A completed test HWE coupling.

are enough to nitrate the lone unsubstituted carbon. Ultimately, after much trial and error, nitration was obtained by exposing **6** to nitrating conditions for 30 mins and then quenching by pouring into a cold NaOH solution. The formation of **1** was confirmed by GC-MS and impure ^{1}H NMR.

In order to carry out the HWE coupling and test the tetramers calculated (Figure 3.1c), four monomers need to be synthesized and purified (**5**, **7**, **8**, **9**) (Scheme 4.3). Monomer **5** was synthesized in the route to producing **1**. Monomer **7** can be easily prepared through reduction of **1** with DIBAL-H. Monomer **9** can be synthesized by the phosphanation of **6** using methods by Barney, et al. followed by nitration.[37] A test HWE coupling between a thiophene monomer and dimethyl 4-cyanobenzylphosphonate, as provided by the Meyer group and used in their HWE coupling reactions, was completed (Scheme 3.3).[33]

Progress was also made towards the necessary phosphonated monomers (**8** and **9**). Starting with thiophene **6**, the bromine moiety was converted to an aldehyde to form **10**, which was then reduced to an alcohol to form **11** (Scheme 3.4).

3.3 EXPERIMENTAL METHODS

Materials. All reagents were used as received without further purification unless otherwise noted. All moisture sensitive reactions were preformed in glassware dried overnight in a 110 °C over under N_2 or Ar. A Bruker Avance III 400MHz spectrometer was used to collect all NMR data. Bruker Topspin 2.0 and iNMR 5.0.9 were used to analyze NMR spectra.

Synthesis of 2-bromo-5-cyano-3-hexyl-4-nitrothiophene (1).[36] To a 10 mL erlen-

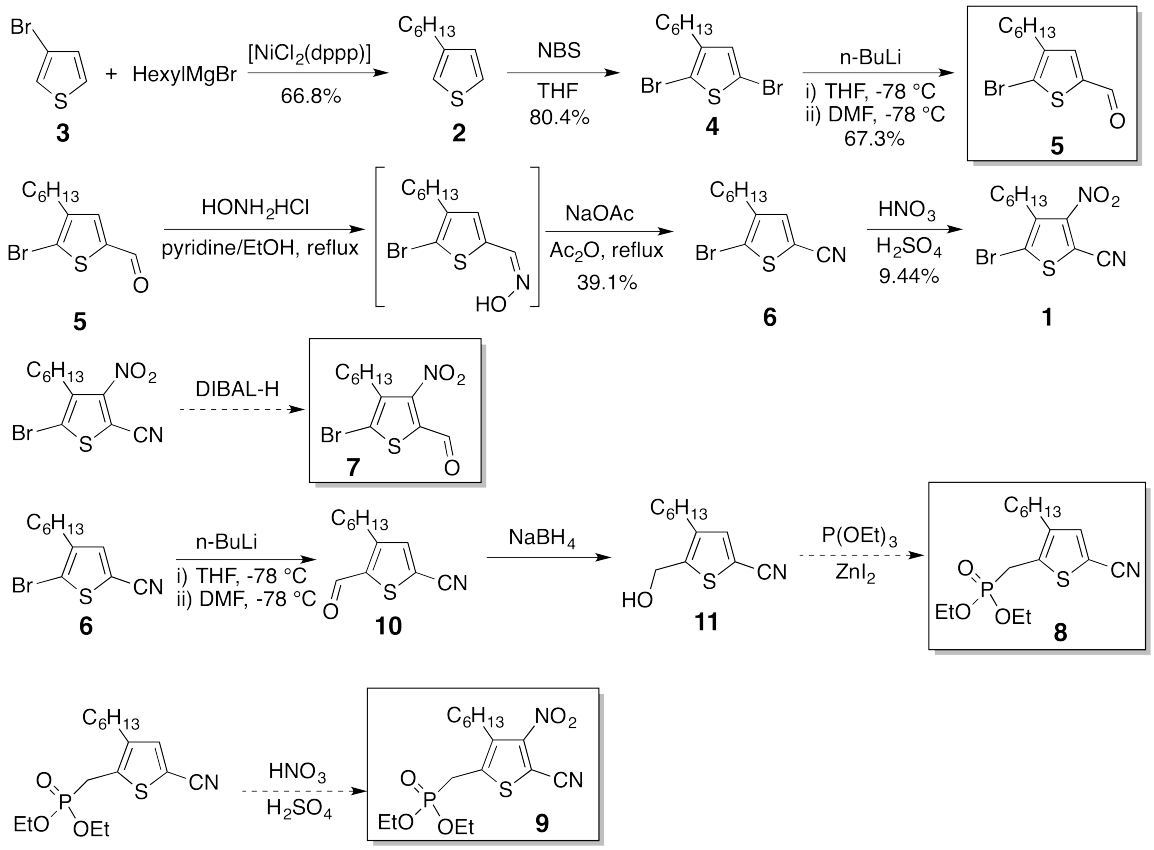

Scheme 3.4: Overall synthetic route for the monomers necessary for HWE coupling.

meyer flask, a solution of 100 mg **6** dissolved in 1 mL H_2SO_4. The solution was chilled in an ice bath and 0.5 mL fuming H_2SO_4 and 0.25 mL fuming HNO_3 were added dropwise. The solution was allowed to sit for 30 min and poured into 75 mL NaOH aq. chilled on ice. The mixture was extracted with $CHCl_3$ 3x and the organic layers were combined and dried *in vacuo*. The crude product was chromatographed on Si_O2 with hexanes-EtOAc (7:3) to afford (**1**) (11 mg, 9.44%). Analysis by GC-MS showed a major peak corresponding to **1** and crude ^{1}H NMR showed peaks corresponding to **1**.

Synthesis of 3-hexylthiophene (2).[34] To a dry, 150 mL three-neck round bottom flask fitted with rubber septa, gas adapter, and a magnetic stirrer under N_2, a solution of **3** (61.3 mmol, 10.0g) in dry diethyl ether was added and the mixture was cooled in an ice bath. Hexylmagnesium bromide (2.0 M in diethyl ether, 67.5 mmol, 33.7 mL) was added dropwise and the mixture was removed from the ice bath. $NiCl_2$(dppp) (0.0705 mmol, 38.2 mg) was added, and the reaction mixture was refluxed overnight. The mixture was cooled to RT, poured into 300 mL 0.5 M HCl and stirred vigerously for 5 min. The layers were separated and the aqueous layer was washed with ether 3x. The organic layers were combined and washed with aq. $NaHCO_3$ 2x, H_2O 2x, and brine 1x. The solvent was removed *in vacuo* The residue was distilled under vacuum (42 °C, 1500 mtorr) to afford **2** (6.89 g, 66.8%) as a yellow liquid: ^{1}H NMR (400 MHz, CDCl3) δ 7.32 (1H, q), 7.01 (2H, q), 2.73 (2H, t), 1.71 (2H, m), 1.42 (6H, m), 1.00 (3H, t) ppm. ^{13}C NMR (100 MHz $CDCl_3$) δ 143.32 (Ar tert), 128.37 (Ar CH), 125.12 (Ar CH), 119.87 (Ar CH), 31.85 (CH_2), 30.69 (CH_2), 30.44 (CH_2), 29.17 (CH_2), 22.77 (CH_2), 14.22 (CH_3) ppm.

Synthesis of 2,5-dibromo-3-hexylthiophene (4).[34] To an Erlenmeyer flask, **2** (41.0 mmol, 6.90 g) was dissolved in 280 mL $CHCl_3$/AcOH (8:2) and then n-bromosuccinimide (86.0 mmol, 15.3 g) was added slowly in portions and the mixture was stirred at RT for 12 h. The reaction mixture was then poured into H_2O and extracted with $CHCl_3$ 3x. The organic layers were combined and washed with 2M NaOH 2x, brine 2x, and then dried *in vacuo*. The residue was distilled under vacuum (85-95 °C, 500 mtorr) to afford **4** (10.6 g, 80.4%) as a yellow oil: ^{1}H NMR (400 MHz, $CDCl_3$) δ 6.81 (1H, s), 2.55 (2H, t), 1.59 (2H, m), 1.35 (6H, m), 0.94 (3H, t) ppm. ^{13}C NMR (100 MHz $CDCl_3$) δ 142.98 (Ar tert), 130.95 (Ar CH), 110.37 (Ar Br), 107.99 (Ar Br), 31.63 (CH_2), 29.60 (CH_2), 29.54 (CH_2), 28.85 (CH_2), 22.63

(CH_2), 14.13 (CH_3) ppm.

Synthesis of 2-bromo-5-formyl-3-hexylthiophene (5).[35] To a dry, 50 mL two-neck round bottom flask fitted with rubber septa, gas adapter, and magnetic stirrer under N_2, a solution of **4** (6.13 mmol, 2.00 g) in 20 mL dry THF was added. The flask was cooled to -78 °C in a dry ice-acetone bath. n-BuLi (1.6 M in Hex., 6.75 mmol, 4.22 mL) was added dropwise over 15 min. After an additional 20 min. DMF (30.7 mmol, 2.37 mL) was added dropwise. The reaction mixture was then gradually warmed up to RT, quenched with H_2O, and extracted with $CHCl_3$ 3x. The organic layers were combined and dried *in vacuo*. The residue was chromatographed on Si_O2 with hexanes-EtOAc (4:1) to afford **5** (1.14 g, 67.3%) as a yellow oil: ^{1}H NMR (400 MHz, $CDCl_3$) δ 9.75 (1H, s), 7.46 (1H, s), 2.59 (2H, t), 1.61 (2H, m), 1.32 (6H, m), 0.89 (3H, t) ppm. ^{13}C NMR (100 MHz $CDCl^3$) δ 181.90 (aldehyde CH), 144.04 (Ar tert), 142.98 (Ar tert), 136.83 (Ar CH), 122.12 (Ar Br), 31.62 (CH_2), 29.55 (CH_2), 29.52 (CH_2), 28.88 (CH_2), 22.64 (CH_2), 14.14 (CH_3) ppm.

Synthesis of 2-bromo-5-cyano-3-hexylthiophene (6).[35] To a 10 mL round bottom flask fitted with a reflux condenser and a magnetic stirrer, a solution of **5** (1.90 mmol, 523 mg) and $NH_2OH{\cdot}HCl$ (2.47 mmol, 172 mg) in 7 mL pyridine-EtOH (50:50). The reaction mixture was stirred and refluxed overnight. After coming to room temperature, the reaction mixture was concentrated and then mixed with H_2O, extracted with $CHCl_3$ 3x. The organic layers were combined and washed with dil. HCl 2x, brine 2x, and were then dried *in vacuo*. To a 10 mL round bottom flask fitted with a reflux condenser and a magnetic stirrer, a solution of the dried intermediate (1.12 mmol, 324.3 mg) and sodium acetate (0.048 mmol, 3.67 mg) in 5 mL acetic anhydride was added. The reaction mixture was stirred and refluxed for 3 h. The reaction mixture was allowed to come to RT and then was poured into dilute NaOH aq. and extracted with $CHCl_3$ 3x. The extracts were washed with brine 2x and dried *in vacuuo*. The residue was chromatographed on Si_O2 with hexanes-EtOAc (4:1) to afford **6** (202.6 mg, 39.1%) as a yellow oil: ^{1}H NMR (400 MHz $CDCl_3$) δ 7.32 (1H, s), 2.58 (2H t), 1.58 (2H, m), 1.31 (6H, m), 0.90 (3H, t) ppm. ^{13}C NMR (100 MHz $CDCl_3$) δ 143.25 (Ar tert), 138.02 (Ar CH), 116.71 (Ar Br), 113.49 (nitrile), 109.40 (Ar nitrile), 31.37 (CH_2), 29.27 (CH_2), 29.15 (CH_2), 28.61 (CH_2), 22.42 (CH_2), 13.93 (CH_3) ppm.

Synthesis of 2-cyano-5-formyl-4-hexylthiopnene (10). To a dry, 25 mL three-neck

round bottom flask fitted with a septa, glas stopper, and gas adapter under Ar, a solution of **6** (0.184 mmol, 50 mg) in 1 mL anhydrous THF. The flask was cooled to -78 °C and t-BuLi (0.221 mmol, 0.13 mL) was added dropwise over 15 min. The reaction mixture was allowed to stir for another 20 min and then DMF (0.920 mmol, 0.013 mL) was added dropwise. The flask was allowed to warm to RT and the mixture was poured into H_2O and extracted with $CHCl_3$. The organic layers were combined and dried in vacuo to afford **10** (35.3 mg, 86.7%). ^{1}H NMR (400 MHz $CDCl_3$) δ 10.09 (1H, s), 7.50 (1H, s), 2.98 (2H, t), 1.67 (2H, m), 1.33 (6H, m), 0.89 ppm (3H, t) ppm.

Synthesis of 2-cyano-4-hexyl-5-(hydroxymethyl)thiophene (11). To a 25 mL round bottom flask, a solution of **10** (0.159 mmol, 35.3 mg) in 1 mL MeOH and 1 mL EtOH. The flask was cooled in an ice bath, $NaBH_4$ (0.319 mmol, 12.1 mg) was added, and the mixture was stirred. Once the bubbling stopped, the mixture was brought to RT and stirred for 4 h. The solvent was removed in vacuo and the residue was extracted with $H_2O/CHCl_3$. The organic layers were combined and the solvent was removed in vacuo to afford **11**.

4.0 PRODOT-ITN D-D COUPLING

4.1 INTRODUCTION

This chapter discusses progress towards the synthesis of the D-D ProDOT-ITN oligomer (Scheme 4.1), which was investigated computationally in Chapter 2. Before synthesizing the monomers necessary to carry out a HWE coupling to match the computational results, Stille coupling was tested as a model system for the ProDOT-ITN oligomer to test the D-D strategy. Stille coupling is straightforward and forms a single bond between an organotin compound and a halide and is catalyzed by platinum.[38] If the D-D strategy looks promising from the Stille coupled oligomers, the necessary monomers will be developed so sequenced ProDOT-ITN tetramers can be made.

4.2 RESULTS AND DISCUSSION

4.2.1 ITN MONOMER

The necessary stannylated-ITN monomer (**12**) was prepared following literature procedure (Scheme 4.2).[39] It should be noted that ITN is very air-sensitive and must be kept under inter atmosphere once it is prepared (starting with **13**).

4.2.2 PRODOT MONOMER

The necessary dibromo-ProDOT monomer (**17**) was prepared following literature procedure (Scheme 4.3).[40]

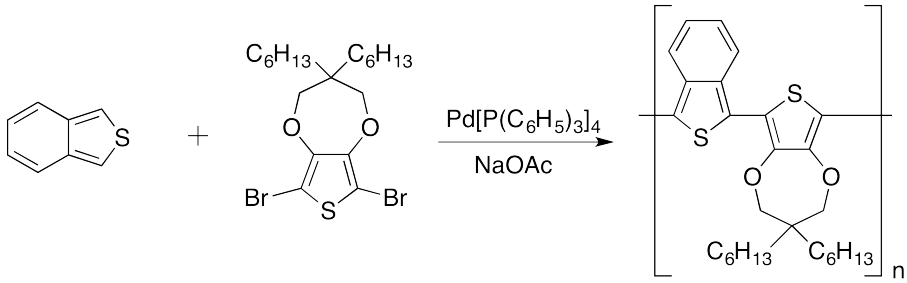

Scheme 4.1: Stille coupling between Sn-ITN and dibromo-ProDOT to form a novel D-D ProDOT-ITN polymer.

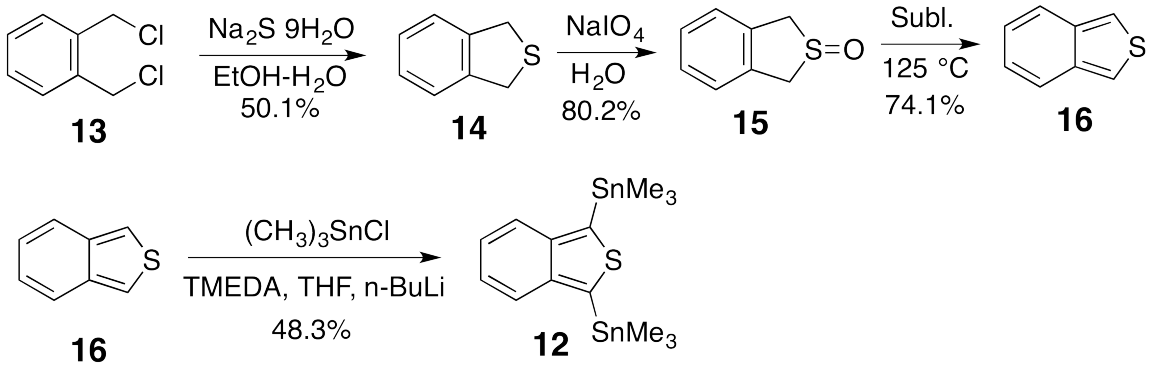

Scheme 4.2: Synthetic procedure to make the stannylated-ITN monomer from literature.

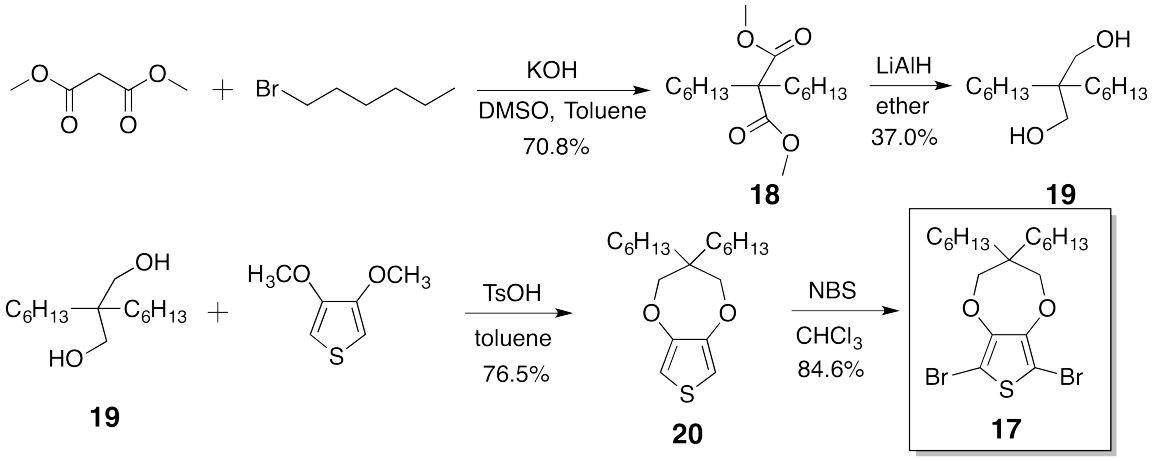

Scheme 4.3: Synthetic procedure to make the dibromo-ProDOT monomer from literature.

4.2.3 D-D PRODOT-ITN OLIGOMERS

The Stille coupling of the prepared ITN and ProDOT monomers was attempted (Scheme 4.1).[39] The coupling reaction is done in a sealed tube in an oven and problems were encountered during this step. Each trial ended with either no coupling or the majority of the time, the tube cracking while in the oven and all the solvent evaporating.

4.3 EXPERIMENTAL METHODS

Materials. All reagents were used as received without further purification unless otherwise noted. All moisture sensitive reactions were preformed in glassware dried overnight in a 110 °C over under N_2 or Ar. A Bruker Avance III 400MHz spectrometer was used to collect all NMR data. Bruker Topspin 2.0 and iNMR 5.0.9 were used to analyze NMR spectra.

Synthesis of 1,3-dihydrobenzo[c]thiophene (14).[39]To a 250 mL round bottom flask, a solution of $Na_2S{\cdot}9H_2O$ (44.1 mmol, 10.6 g) in 100 mL EtOH and 30 mL H_2O was added. A Soxhlet extractor (glass fritted thimble) with 1,2-bischloromethylbenzene (**11**) (29.4 mmol, 5.14 g) was fitted to the flask and the extraction was run for 4 h. The solvent was removed

in vacuo and the crude mixture was extracted with DCM and H_2O. The DCM layers were combined and dried *in vacuo* to afford **14** as a clear oil with some impurities (4.24g). ^{1}H NMR (400 MHz $CDCl_3$) δ 7.26 (4H, m), 4.30 (4H, s) ppm. ^{13}C NMR (100 MHz $CDCl_3$) δ 140.48 (Ar tert), 126.84 (Ar CH), 124.81 (Ar CH), 38.19 (CH_2) ppm.

Synthesis of 1,3-Dihydrobenzo[c]thiophene-2-oxide (15).[39] To a 250 mL round bottom flask, a solution of **14** (31.1 mmol, 4.24g) in 100 mL EtOH was cooled in an ice bath. A solution of sodium periodate (31.1 mmol, 6.65 g) in 80 mL H_2O was added dropwise while stirring the solution vigerously for 3h. The reaction mixture was allowed to come to RT and a white inorganic salt was filtered off. The solvent was removed *in vacuo* to afford **15** (3.80 g, 80.2%). ^{1}H NMR (400 MHz $CDCl_3$) δ 7.35 (4H, m), 4.23 (4H, dd) ppm. ^{13}C NMR (100 MHz $CDCl_3$) δ 135.20 (Ar tert), 128.57 (Ar CH), 126.71 (Ar CH), 59.48 (CH_2) ppm.

Synthesis of 1,3-bis(trimethylstannyl)benzo[c]thiophene (Sn-ITN) (12).[39] To neutral, activated alumina (3 g) in a sublimator, **15** (9.9 mmol, 1.5 g) was added. The sublimator was heated to 105-125 °C for 4 h. Product **16** was deposited on the cold finger as a white solid (7.30 mmol, 0.98 g, 74.1%). To a dry, 50 mL three-neck round bottom flask fitted with a septa, gas port, and glass stopper under N_2, a solution of 11 (2.98 mmol, 400 mg) in 10 mL anhydrous THF was added. The flask was cooled in an ice bath and n-BuLi (1.6 M in hex.) (7.16 mmol, 4.48 mL) was added dropwise. The flask was allowed to come to RT and stir for 2 h. The mixture was cooled to -78 °C and trimethyltin chloride (1.0 M in THF) (7.46 mmol, 7.46 mL) was added dropwise. The flask was allowed to come to RT and was stirred overnight. The reaction mixture was poured into 20 mL sat. NH_4HCO_3 and separated. The aqueous phase was extracted with ether 2x and all organic phases were combined and washed with H_2O 3x and dried over $MgSO_4$. The solvent was removed *in vacuo* to give **12** as a dark yellow oil (662.3 mg, 48.3%). ^{1}H NMR (400 MHz $CDCl_3$) δ 7.68 (2H, dd, J = 3.1, 6.7 Hz), 7.08 (2H, dd, J = 3.1, 6.7 Hz), 0.50 (18H, s) ppm. ^{13}C NMR (100 MHz $CDCl_3$) δ 146.80 (Ar CH), 137.06 (Ar Sn), 124.00 (Ar CH), 122.75 (Ar tert), -10.23 ($Sn[CH_3]_3$) ppm.

Synthesis of dimethyl dihexylmalonate (18).[40] To a 250 mL round bottom flask, a solution of pulverized KOH pellets (114 mmol, 6.40g) in 75 mL toluene and 75 mL DMSO was added and stirred for 30 min. Then dimethyl malonate (37.9 mmol, 5.00g) and 1-

bromohexane (151 mmol, 25.0 g) were added and the mixture was stirred overnight. The reaction mixture was poured into 150 mL H_2O and extracted with ether. The organic layers were combined and concentrated. The crude mixture was purified via vacuum distillation (125-138 °C) to afford **18** as a clear oil (8.07g, 70.8%). ^{1}H NMR (400 MHz $CDCl_3$) δ 3.66 (6H, s), 1.82 (4H, m), 1.23 (12H, m), 1.01 (4H, m), 0.83 (6H, t) ppm. ^{13}C NMR (100 MHz $CDCl_3$) δ 172.50 (ester), 57.74 (quat C), 52.22 (ester CH_3), 32.52 (CH_2), 31.59 (CH_2), 29.55 (CH_2), 24.05 (CH_2), 22.62 (CH_2), 14.07 (CH_3) ppm.

Synthesis of 2,2-dihexylpropane-1,3-diol (19).[40] To a dry, 100 mL 2-neck round bottom flask fitted with a septa and a gas port under N_2, a solution of LiAlH (15.0 mmol, 0.568 g) and **18** (9.98 mmol, 3.00 g) in 40 mL anhydrous ether was added and stirred overnight. The reaction was quenched with H_2O and extracted with ether. The solvent was removed in vacuuo to provide **19** as a clear liquid (903.6 mg, 37.0%). ^{1}H NMR (400 MHz $CDCl_3$) δ 3.47 (4H, s), 3.23 (2H, s), 1.22 (20H, m), 0.86 (6H, t) ppm. ^{13}C NMR (100 MHz $CDCl_3$) δ 69.07 (alcohol CH_2), 41.04 (tert C), 31.93 (CH_2), 30.80 (CH_2), 30.37 (CH_2), 22.90 (CH_2), 22.79 (CH_2), 14.18 (CH_3) ppm.

Synthesis of 3,3-dihexyl-3,4-dihydro-2H-thieno[3,4-b][1,4]-dioxepine (dihexyl-ProDOT, 20).[40] To a 50 mL, three-neck round bottom flask fitted with two glass stoppers and a reflux condenser, a solution of 14 (1.85 mmol, 452 mg), p-toluenesulfonic acid (0.185 mmol, 35.2 mg), and 3,4-dimethoxythiophene (1.87 mmol, 269 mg) in 10 mL toluene was added. The reaction mixture was stirred and refluxed overnight. The mixture was washed with H_2O (3x) and the organic layer was dried in vacuo to afford **20** as a black solid (484.2 mg, 76.5%). ^{1}H NMR (400 MHz $CDCl_3$) ° 6.42 (2H, s), 3.94 (4H, s), 1.29 (20H, m), 0.89 (6H, m) ppm. ^{13}C NMR (100 MHz $CDCl_3$) δ 149.88 (Ar tert), 104.76 (Ar CH), 76.74 (CH_2), 43.88 (tert), 32.04 (CH_2), 31.87 (H_2), 30.28 (CH_2), 22.92 (CH_2), 22.78 (CH_2), 14.19 (CH_3) ppm.

Synthesis of 6,8-dibromo-3,3-dihexyl-3,4-dihydro-2H-thieno[3,4-b]- [1,4]dioxepine (dibromo-dihexyl-ProDOT, 17).[40] To a 250 mL Erlenmeyer flask, a solution of 14 (1.49 mmol, 484 mg) in 60 mL chloroform was added and stirred for 30 min. N-bromosuccinimide (4.48 mmol, 797 mg) was added over 15 min and the reaction mixture was stirred overnight. The mixture was washed with H_2O (3x) and the organic layer was

dried in vacuo to afford **17** as a black solid (607.7 mg, 84.6%). ^{1}H NMR (400 MHz $CDCl_3$) δ 3.90 (4H, s), 1.36 (4H, m) 1.30 (16H, m), 0.88 (6H, t) ppm. ^{13}C NMR (100 MHz $CDCl_3$) δ 147.24 (Ar tert), 90.74 (Ar Br), 78.11 (CH_2), 44.10 (tert) 31.83 (CH_2), 31.71 (CH_2), 30.16 (H_2), 22.79 (CH_2), 22.76 (CH_2), 14.21 (CH_3) ppm.

5.0 CONCLUSIONS

Conjugated polymers have shown enormous promise for commercial solar cells. With their inexpensive raw materials, ease of processing, and ability to be flexible and/or transparent, they will be cheaper and more versatile than the current generation of inorganic, silicon solar cells. This work focuses on developing new D-A and D-D conjugated polymers as well as the elucidation of the sequence effect.

The immediate goals in this project are the synthesis of the NT monomer, synthesis of PV-NTV oligomers, and the ProDOT-ITN coupling. The only issue remaining with the NT monomer is purification. Once the NT monomer purification is worked out, the reactions for the other three required monomers can be completed. Once enough pure product is obtained, the synthesys of the sequenced PV-NTV tetramers (D-A) using HWE coupling can be carried out. A test coupling reaction between a non-nitrated thiophene monomer and the PV monomer from the Meyer group has been completed to show that the coupling works with substituted thiophenes. After preparing some of the sequenced tetramers and experimentally determining their band gaps, the results will be compared to the computational results. Good agreement will show that it is indeed possible to span 1 eV just by changing the sequence of a tetramer.

For the ProDOT-ITN (D-D) coupling, the conditions for the Stille coupling need to be optimized and the issue of the sealed reaction tube cracking solved. It has been suggested to our group that direct (hetero)arylation might be a viable alternative to the Stillie coupling of the ProDOT-ITN system.[41] The coupling of EDOT and a dibromo-substituted fluorene has been demonstrated by Yamazaki, et al.[42] Completion of this coupling will show that is possible to couple these two donor monomers and provide an opportunity to experimentally investigate the electronic properties of a D-D oligomer or polymer. From there, the appro-

priate monomers for HWE coupling can be developed and sequenced tetramers synthesized. The electronic properties of the tetramers can then be experimentally determined and compared to the computational results. This will allow confirmation that the sequence effect also holds for D-D polymers and can be utilized to tune the band gap over a 1 eV range. There is only one known report in the literature of D-D conjugated polymers for solar cells.[43] Kozycz, et. al. utilize a block-copolymer motif and do not investigate any other sequences, making this alternating (and future sequenced) D-D polymers unique in the field. D-D type conjugated polymers could prove to push PSC efficiency above 10% and beyond, as predicted in our groups previous work.[24,25]

In addition to the current two systems focused on in this work, the synthesis of additional D-A and D-D tetramers based on top monomers from the screening will allow the development of a library of novel, synthetically tractable monomers as well as the tools necessary to synthesize sequenced tetramers. By studying the optoelectronic properties of multiple sequenced tetramer systems, it can be shown that the sequence of a polymer can significantly affect its viability for an n-type PSC material.

On a larger scale, by feeding the experimental data from this project back into the groups ongoing screening effort, we can better predict future monomer targets, saving synthetic effort and money. New promising monomers from the screening will be synthesized and tested, allowing for a continuous feedback loop. By using this iterative method of selecting new synthetic targets and unique combination of theory and experiment, we will be able to determine what brings about the sequence effect. Do certain moieties cause certain changes in electronic structure? Is there a way to empirically predict HOMO and LUMO levels as well as band gap based on the structure of a molecule? We have begun to unravel the answers to these questions in our recent Perspective paper.[25] For example, some monomers were found that always have the same effect on HOMO, LUMO, and/or band gap, regardless of the other monomer. We also looked at twelve diverse monomers and generated all possible tetramer combinations. Through statistical analysis, we were able to show a clear modulation of the HOMO, LUMO, and band gap by monomer sequence.

Novel conjugated polymers developed in this work could find uses in organic electronics such as PSCs, organzic light emitting devices (OLEDs), and organic field effect transistors

(OFETs). Since OLEDs and PSCs can be printed over a large area, while remaining flexible, transparent, and lightweight, unique applications such as rollable screens, OLED light panels to replace fluorescent lighting, and PSCs on window glass are possible. While much work has already been done in this field, the relatively unexplored realm of D-D polymers and the elucidation of the sequence effect provide opportunity for innovation and the improvement of PSC efficiency.

BIBLIOGRAPHY

[1] Darling, S.; You, F. *RSC Adv.* **2013**, DOI: 10.1039–C3RA42989J.

[2] Gelman, R. *2011 Renewable Energy Data Book*; 2012.

[3] Lopez, A.; Roberts, B.; Heimiller, D.; Blair, N.; Porro, G. *U.S. Renewable Energy Technical Potentials: A GIS-Based Analysis*; 2012.

[4] Tang, C. W. *Appl. Phys. Lett.* **1986**, *48*, 183.

[5] Cheng, Y.-J.; Yang, S.-H.; Hsu, C.-S. *Chem. Rev.* **2009**, *109*, 5868–5923.

[6] Li, G.; Zhu, R.; Yang, Y. *Nature Photon.* **2012**, *6*, 153–161.

[7] Wang, Y.; Wei, W.; Liu, X.; Gu, Y. *Sol. Energ. Mat. Sol. Cells* **2012**, *98*, 129–145.

[8] Zhou, H.; Yang, L.; You, W. *Macromolecules* **2012**, *45*, 607–632.

[9] Duan, C.; Huang, F.; Cao, Y. *J. Mater. Chem.* **2012**, *22*, 10416–10434.

[10] Thompson, B. C.; Fréchet, J. M. J. *Angew. Chem. Int. Ed.* **2008**, *47*, 58–77.

[11] Heeger, A. J. *Chem. Soc. Rev.* **2010**, *39*, 2354–2371.

[12] Sariciftci, N. S.; smilowitz, L.; Heeger, A. J.; Wudl, F. *Science* **1992**, *258*, 1474–1476.

[13] Morita, S.; Zakhidov, A. A.; Yoshino, K. *Synthetic Metals* **1992**, *82*, 249–252.

[14] Sommer, M.; Huettner, S.; Thelakkat, M. *J. Mater. Chem.* **2010**, *20*, 10788–10797.

[15] Chen, T. A.; Rieke, R. D. *J. Am. Chem. Soc.* **1992**, *114*, 10087–10088.

[16] McCullough, R. D.; Tristram-Nagle, S.; Williams, S. P.; Lowe, R. D.; Jayaraman, M. *J. Am. Chem. Soc.* **1993**, *115*, 4910–4911.

[17] McCullough, R. D.; Lowe, R. D.; Jayaraman, M.; Anderson, D. L. *J. Org. Chem.* **1993**, *58*, 904–912.

[18] He, Z.; Zhong, C.; Su, S.; Xu, M.; Wu, H.; Cao, Y. *Nature Photon.* **2012**, *6*, 593–597.

[19] Li, Y. *Acc. Chem. Res.* **2012**, *45*, 723–733.

[20] Potscavage, W. J., Jr.; Sharma, A.; Kippelen, B. *Acc. Chem. Res.* **2009**, *42*, 1758–1767.

[21] Scharber, M. C.; Mühlbacher, D.; Koppe, M.; Denk, P.; Waldauf, C.; Heeger, A. J.; Brabec, C. J. *Adv. Mater.* **2006**, *18*, 789–794.

[22] Duan, C.; Huang, F.; Cao, Y. *J. Mater. Chem.* **2012**, *22*, 10416–10434.

[23] Zhang, Z.-G.; Wang, J. *J. Mater. Chem.* **2012**, *22*, 4178–4187.

[24] O'Boyle, N. M.; Campbell, C. M.; Hutchison, G. R. *J. Phys. Chem. C* **2011**, *115*, 16200–16210.

[25] Kanal, I. Y.; Owens, S. G.; Bechtel, J. S.; Hutchison, G. R. *J. Phys. Chem. Lett.* **2013**, 1613–1623.

[26] O'Boyle, N. M.; Banck, M.; James, C. A.; Morley, C.; Vandermeersch, T.; Hutchison, G. R. *J. Cheminf.* **2011**, *3*, 33.

[27] Halgren, T. A. *J. Comput. Chem.* **1996**, *17*, 553–586.

[28] Halgren, T. A. *J. Comput. Chem.* **1996**, *17*, 520–552.

[29] Halgren, T. A.; Nachbar, R. B. *J. Comput. Chem.* **1996**, *17*, 587–615.

[30] Frisch, M. J. et al. Gaussian 09 Revision A.1. Gaussian Inc. Wallingford CT 2009.

[31] Kiya, Y.; Hutchison, G. R.; Henderson, J. C.; Sarukawa, T.; Hatozaki, O.; Oyama, N.; Abruña, H. D. *Langmuir* **2006**, *22*, 10554–10563.

[32] Wadsworth, W.; Emmons, W. *J. Am. Chem. Soc.* **1961**, *83*, 1733–1738.

[33] Norris, B. N.; Zhang, S.; Campbell, C. M.; Auletta, J. T.; Calvo-Marzal, P.; Hutchison, G. R.; Meyer, T. Y. *Macromolecules* **2013**, *46*, 1384–1392.

[34] Loewe, R. S.; Ewbank, P. C.; Liu, J.; Zhai, L.; McCullough, R. D. *Macromolecules* **2001**, *34*, 4324–4333.

[35] Hayashi, N.; Nishihara, T.; Matsukihira, T.; Nakashima, H.; Miyabayashi, K.; Miyake, M.; Higuchi, H. *Bull. Chem. Soc. Jpn.* **2007**, *80*, 371–386.

[36] Mozingo, R.; Harris, S.; Wolf, D. *J. Am. Chem. Soc.* **1945**, *67*, 2092–2095.

[37] Barney, R. J.; Richardson, R. M.; Wiemer, D. F. *J. Org. Chem.* **2011**, *76*, 2875–2879.

[38] Stille, J. K. *Angew. Chem. Int. Ed.* **1986**, *25*, 508–524.

[39] Kawabata, K.; Goto, H. *J. Mater. Chem.* **2012**, *22*, 23514.

[40] Nielsen, C. B.; Bjørnholm, T. *Macromolecules* **2005**, *38*, 10379–10387.

[41] Mercier, L. G.; Leclerc, M. *Acc. Chem. Res.* **2013**, *46*, 1597–1605.

[42] Yamazaki, K.; Kuwabara, J.; Kanbara, T. *Macromol. Rapid Commun.* **2012**, *34*, 69–73.

[43] Kozycz, L. M.; Gao, D.; Hollinger, J.; Seferos, D. S. *Macromolecules* **2012**, *45*, 5823–5832.